Am J Cancer Res 2022;12(2):839-851
www.ajcr.us /ISSN:2156-6976/ajcr0133111

Original Article

Depletion of CCN1/CYR61 reduces triple-negative/basal-like breast cancer aggressiveness

Ingrid Espinoza[1,11,12*], Chandra Kurapaty[1*], Cheol-Hong Park[1], Travis Vander Steen[1], Celina G Kleer[2], Elizabeth Wiley[3], Alfred Rademaker[4], Elisabet Cuyàs[5,6], Sara Verdura[5,6], Maria Buxó[7], Carol Reynolds[8], Javier A Menendez[5,6], Ruth Lupu[1,9,10]

[1]Division of Experimental Pathology, Department of Laboratory Medicine and Pathology, Mayo Clinic, Rochester, MN 55905, USA; [2]Department of Pathology, University of Michigan, Ann Arbor, MI 48109, USA; [3]Department of Pathology, University of Illinois at Chicago, Chicago, IL 60607, USA; [4]Department of Preventive Medicine, Northwestern University Feinberg School of Medicine, Chicago, IL 60611, USA; [5]Girona Biomedical Research Institute, 17190 Salt, Girona, Spain; [6]Program Against Cancer Therapeutic Resistance (ProCURE), Metabolism & Cancer Group, Catalan Institute of Oncology, 17007 Girona, Spain; [7]Statistical and Methodological Advice Unit, Girona Biomedical Research Institute, 17190 Salt, Girona, Spain; [8]Department of Pathology, Division of Anatomic Pathology, Mayo Clinic, Rochester, MN 55905, USA; [9]Mayo Clinic Cancer Center, Rochester, MN 55905, USA; [10]Department of Biochemistry and Molecular Biology Laboratory, Mayo Clinic Minnesota, Rochester, MN 55905, USA; [11]Department of Preventive Medicine, John D. Bower School of Population Health, University of Mississippi Medical Center, Jackson, MS 39216, USA; [12]Cancer Institute, School of Medicine, University of Mississippi Medical Center, Jackson, MS 39216, USA. [*]Equal contributors.

Received March 14, 2021; Accepted February 3, 2022; Epub February 15, 2022; Published February 28, 2022

Abstract: Triple-negative/basal-like breast cancer (BC) is characterized by aggressive biological features, which allow relapse and metastatic spread to occur more frequently than in hormone receptor-positive (luminal) subtypes. The molecular complexity of triple-negative/basal-like BC poses major challenges for the implementation of targeted therapies, and chemotherapy remains the standard approach at all stages. The matricellular protein cysteine-rich angiogenic inducer 61 (CCN1/CYR61) is associated with aggressive metastatic phenotypes and poor prognosis in BC, but it is unclear whether anti-CCN1 approaches can be successfully applied in triple-negative/basal-like BC. Herein, we first characterized the prevalence of CNN1 expression in matched samples of primary tumors and metastatic relapse in a series of patients with BC. We then investigated the biological effect of CCN1 depletion on tumorigenic traits *in vitro* and *in vivo* using archetypal TNBC cell lines. Immunohistochemical analyses of tissue microarrays revealed a significant increase of the highest CCN1 score in recurrent tissues of triple-negative/basal-like BC tumors. Stable silencing of *CCN1* in triple-negative/basal-like BC cells promoted a marked reduction in the expression of the CCN1 integrin receptor $\alpha_v\beta_3$, inhibited anchorage-dependent cell growth, reduced clonogenicity, and impaired migration capacity. In an orthotopic model of triple-negative/basal-like BC, silencing of *CCN1* notably reduced tumor burden, which was accompanied by decreased microvessel density and concurrent induction of the luminal epithelial marker E-cadherin. Thus, CNN1/CYR61-targeting strategies might have therapeutic value in suppressing the biological aggressiveness of triple-negative/basal-like BC.

Keywords: CCN1, breast cancer, metastasis, triple-negative, basal-like, integrins

Introduction

Triple-negative breast cancer (TNBC) is a subgroup of BC clinically defined by the lack of expression of the estrogen receptor (ER), the progesterone receptor (PR) and human epidermal growth factor receptor 2 (HER2). Basal-like breast carcinomas, which express cytokeratins and other non-luminal (basal) genes, exhibit the greatest overlap with TNBC [1-5]. Compared with hormone receptor-positive (luminal) BC subtypes, triple-negative/basal-like BC carries a dismal prognosis, and has a higher propensity to earlier metastases with shorter survival after recurrence. The absence of the three major receptors involved in BC progression, the biological complexity of a highly heterogenous disease, and the lack of recurrent targetable

genetic alterations, altogether poses major challenges for the implementation of novel strategies to combat triple-negative/basal-like BC [6-9]. Not surprisingly, systemic chemotherapy, rather than targeted therapy, remains the standard therapeutic approach for triple-negative/basal-like BC at all stages. Discovery and validation of druggable molecular targets that can provide new therapeutic strategies to limit the progression and metastatic behavior of invasive triple-negative/basal-like BC remains a clinical aspiration.

CCN1 (also named cysteine-rich angiogenic inducer 61 [CYR61]), an archetypal component of the so-called CCN (CYR61, CTGF, NOV) family of matricellular proteins [10-13], has been identified as a potential contributing factor to the pathogenesis of triple-negative/basal-like BC [14-18]. CCN1 is a secreted cysteine-rich, heparin-binding protein that associates with the cell surface and the extracellular matrix (ECM). During embryonic development and in some pathophysiological contexts such as inflammation, wound healing, and tissue repair, CCN1 can mediate a multifaceted repertoire of functions, namely cell adhesion and migration, growth factor-induced DNA synthesis, cell survival, angiogenesis, and chemotaxis in fibroblasts, endothelial cells, and mesenchymal cells (reviewed in [19] and [20]). When aberrantly expressed in cancer cells, CCN1 is not only a powerful angiogenic inducer, but also promotes cell proliferation and survival, invasion, and metastasis [21-23]. Accordingly, BC-associated CCN1 expression has been shown to correlate with higher clinical stage, larger tumor size, lymph node positivity, and poorer prognosis [24, 25]. Intriguingly, there appears to be a close association between increased CCN1 expression and aggressiveness in highly invasive and metastatic triple-negative/basal-like BC cells [21-23]. Moreover, CCN1 expression can promote hormone-independence and antiestrogen-resistance in ER-positive BC cells, pointing to a negative link between CCN1 expression and ER status and function in BC [21-26]. However, despite the clear association between CCN1 and aggressiveness in BC, it remains unknown whether CCN1-targeted approaches might be of therapeutic relevance in triple-negative/basal-like BC.

Herein, we analyzed the prevalence of CNN1 expression in matched pairs of primary tumor and recurrent/metastatic relapses in a series of patients with BC. We then examined the effects of CCN1 on cellular proliferation, anchorage-independent clonal capacity, migration, and tumorigenic traits in CCN1-depleted derivatives of archetypal triple-negative/basal-like BC cells. The results definitely points CCN1 as a key signaling node eliciting the biological aggressiveness of triple-negative/basal-like BC.

Materials and methods

Human breast cancer tissue microarrays

Tissue microarrays (TMAs) consisting of primary tumor (n=147) and recurrent/metastatic relapses (n=120) from a series of BC patients was supplied by the Northwestern Breast SPORE at Northwestern University (Chicago, IL). TMAs were generated from women with invasive carcinomas and controls. Each TMA included three different cores from each tumor, and also included three tissue cores from each normal breast tissue (reduction mammoplasties), breast stroma, and other carcinomas (e.g., liver, lung, ovary and kidney). The TMAs were designed and prepared by Dr. Elizabeth Wiley (Professor and Director, Surgical Pathology University of Illinois Medical Center, Chicago). Scoring of the TMAs for CCN1/CYR61 expression was performed by Dr. Carol Reynolds, a board-certified breast pathologist at Mayo Clinic in Rochester, MN, who was blinded to clinical parameters.

Cell lines and cell culture

The triple-negative/basal-like BC cell lines MDA-MB-231, BT-549, and Hs578T were acquired from the American Type Culture Collection (Manassas, VA) and maintained in phenol red-containing improved Iscove's modified Eagle's medium (IMEM; Biosource International, Camarillo, CA) containing 5% (*v/v*) heat-inactivated fetal bovine serum (FBS) and 2 mmol/L L-glutamine. Cells were maintained at 37°C in a humidified atmosphere of 95% air and 5% CO_2. Cells were authenticated and identified using short tandem repeat profiling (Genotyping Shared Resource, Mayo Clinic Rochester). Cells were regularly tested to confirm the absence of mycoplasma using the MycoAlert® Mycoplasma Detection Kit (Lonza, Walkersville, MD).

Generation of CCN1-silenced cell lines

MDA-MB-231, BT-549, and Hs578T cells were infected with a lentiviral pLKO.1 vector (V) construct or the pLKO.1 vector containing validated shRNAs targeting *CCN1* at a multiplicity of infection 5 (TRCN0000118100 & NM_001554.3-1310s1c1) for 24 h (Sigma-Aldrich, Saint Louis, MO). After transduction, the medium containing the lentivirus was removed and replaced with fresh medium containing puromycin (0.75 μg/mL). Antibiotic selection was sustained for up to 3 weeks to generate the stable *CCN1*-silenced cell lines.

Immunoblotting

Cell lysates were prepared by harvesting the cells in 1× Cell Lysis Buffer (Cell Signaling Technology, Danvers, MA) containing protease and phosphatase inhibitors (Roche, Nutley, NJ) for 30 min on ice with vortexing every 5 min. Conditioned medium was prepared from cells grown in 6-well plates with IMEM containing 5% FBS for 24 h and then maintained in serum-free medium for 24 h. After starvation, the medium was collected, centrifuged and the supernatant was referred to as conditioned medium. Protein concentration was determined using the Pierce® BCA protein assay kit (Pierce, Rockford, IL). Ten μg of pooled proteins were resolved by 10% polyacrylamide gel electrophoresis (Criterion XT Bis-Tris precast Gel; Bio-Rad, München, Germany) and analyzed by immunoblotting for CCN1 using the primary polyclonal rabbit anti-Cyr61 (H78) antibody (1:1,000) (Santa Cruz Biotechnology, Santa Cruz, CA). Blots were then incubated with a 1:4,000 dilution of horseradish peroxidase-conjugated goat anti-rabbit IgG secondary antibody (Cell Signaling Technology). Blots were reprobed with a monoclonal antibody for β-actin (1:25,000) (Santa Cruz Biotechnology) and signals were detected using a 1:4,000 dilution of a horseradish peroxidase-conjugated goat anti-mouse IgG secondary antibody. All antibody dilutions were prepared in 5% non-fat dry milk in Tris-buffered saline (Cellgro, Mediatech, Inc., Herndon, VA) with 0.1% Tween-20 (Sigma-Aldrich). Proteins were detected by the enhanced chemoluminescence (ECL) reaction using the Amersham Hyperfilm ECL (Amersham-Pharmacia, Piscataway, NJ).

Flow cytometry evaluation of $\alpha_v\beta_3$ integrin expression

Following serum starvation, cells were detached by scrapping, counted, and incubated with a monoclonal antibody against the RGD-binding integrin $\alpha_v\beta_3$ clone LM609 (3 μg/500×10^3 cells/100 μL) (Chemicon International, Temecula, CA). Samples were then washed twice with cold phosphate buffered saline (PBS) containing 1% FBS, and incubated with an FITC-conjugated secondary antibody (1:200) (Jackson Immunoresearch, Avondale, PA) for 30 min at 4°C. Cells were then analyzed on an Accuri C6 flow cytometer (Accuri Cytometers, Inc., Ann Arbor, MI). Data acquisition and analysis were performed using BD Accuri™ C6 Plus software (Version 1.01.202.1).

In vitro cell growth assays

To evaluate anchorage-dependent cell growth, cells (5×10^3) were seeded in 24-well plates (Cellstar, Greiner Bio-One GmbH, Essen, Germany). After 24 h, cells were counted every day for 4 days using the Vi-cell XR cell viability analyzer (Beckman Coulter, Miami, FL). To evaluate cell growth in anchorage-independent conditions, cells were grown in soft agar. Briefly, a bottom layer of 1.5 ml of DMEM: Ham's F-12 medium containing 0.6% agar and 5% FBS was prepared in a 6-well plate. After solidification of the bottom layer, cells (1×10^4/well) were suspended in a 1-mL top layer of Dulbecco's modified Eagle's medium (DMEM): Ham's F-12 medium containing 0.35% agar and 5% FBS. Plates were then incubated in a humidified 5% CO_2 incubator at 37°C. After 9 days, colonies larger than 50 μm in diameter were counted with an automatic counter (Gel count, Oxford Optronix, Milton, UK).

Cell migration assays

Cell migration was monitored using scratch wound healing assays. Briefly, cells were seeded in 6-well plates and incubated in a humidified 5% CO_2 incubator at 37°C. At >90% cell confluence, a wound was made by making a scratch with a pipette tip of 200 μL and the wells were washed thoroughly with PBS three times. Cells were then incubated in serum-free IMEM during the time span of the wound healing. An image for each scratch was taken in the same region at 0 h and 18 h and wound healing

images were analyzed using Scion Image software (Scion Corporation, Frederick, MD).

Enzyme-linked immunosorbent assay analysis of secreted vascular endothelial growth factor

Cells (2×10^5/well) were seeded in 6-well plates in complete growth medium. Upon reaching 70% confluence, the cells were washed twice with PBS and cultured in serum-free medium. After 24 h of starvation, culture medium was collected, centrifuged at 1100×*g* for 10 min at 4°C to remove debris, and stored at -80°C until analysis. Conditioned medium levels of vascular endothelial growth factor (VEGF) were determined with an enzyme-linked immunosorbent assay (ELISA) kit (Peprotech, Rocky Hill, NJ). Absorbance was measured at 405 nm by an ELISA reader (Bio-Tek Instruments, Winooski, VT) and levels were normalized by total protein in the corresponding cell lysates.

In vivo studies

Xenografts were established by direct injection of 2×10^6 cells (in 100 µL of PBS) subcutaneously into the left and right mammary fat pad of 3- to 4-week-old athymic female nude-Doxn1^{nu} mice (Harlan Sprague Dawley, Madison, WI, USA) (n=12 per group). Tumor volume values were calculated using a Vernier caliper with the formula: tumor volume (mm^3) = (length × width × height)/2. Mice were euthanized at completion of the experiment or when tumors reached a volume of 1000 mm^3 in accordance with IACUC protocols. Tumor tissues were removed, fixed in formalin, and embedded in paraffin for histochemical analysis.

Immunohistochemical analyses

Paraffin-embedded tissues were deparaffinized by incubating slides at 60°C for 60 min followed by three series of dehydration/hydration with xylene and graded alcohols. Antigen retrieval was carried out either by incubating slides in a target retrieval citrate buffer (pH 6.0) (DakoCytomation, Carpinteria, CA) at 95°C for 15 min for E-cadherin and vimentin, or by incubating slides with proteinase K (DakoCytomation) for 10 min at room temperature for CD31. Sections were then rinsed with PBS and treated with 3% H_2O_2 in distilled water for 15 min to block endogenous peroxidase activity. Non-specific antibody binding was minimized by incubating the sections with normal horse serum for 30 min. The sections were then incubated with the following primary antibodies: E-cadherin (1:300) for 1.5 h at room temperature, or vimentin (1:500) and CD31 (1:700) overnight at 4°C. On the next day, the slides were incubated with an anti-rabbit and anti-mouse biotin-labeled secondary antibody (DakoCytomation) followed by incubation with streptavidin-biotin-peroxidase for 30 min each at room temperature. The immunoprecipitate was visualized using the DAB+ Kit (DakoCytomation) and counterstained with hematoxylin.

Statistical analysis

Cell-based assays: Three independent biological experiments with n≥3 technical replicates were performed foe each sample. Data are presented as mean ± S.D. Comparisons of means of ≥3 groups were performed by one-way analysis of variance (ANOVA) followed by Tukey's multiple comparisons tests using SPSS (release 2017, v25.0; IBM Corp., Armonk, NY, USA) and STATA (release 2013; StataCorp LP, College Station, TX, USA). All statistical tests were two-sided and *P*-values <0.05 and <0.005 were considered to be statistically significant and highly significant (denoted as * and **, respectively).

Patients: Contingency tables were constructed for categorical parameters presented as frequencies (N, %), and were compared using a chi-squared test (or Fisher's exact test, when appropriate). The Cochran-Mantel-Haenszel test was used to measure the association between "primary vs recurrent/metastatic" and "CCN1 score" across breast cancer molecular subtypes. Post-hoc tests were carried out when appropriate. Statistical analyses were conducted using SPSS 26.0 (IBM Corp. Released 2019. IBM SPSS Statistics for Windows, Version 26.0. Armonk, NY: IBM Corp) and R Statistical Software (4.1.1; R Core Team 2021) using the package "rcompanion" (R package version 2.4.1. https://CRAN.R-project.org/package=rcompanion).

Results

CCN1 is more commonly overexpressed in relapsed triple-negative/basal-like BC

To address the clinical relevance of CCN1/CYR61 in BC, we assessed CCN1/CYR61

Table 1. Baseline clinicopathological features of BC patients

	All samples *N*=267 (%)	Primary *N*=147 (%)	Relapsed/Metastatic *N*=120 (%)	*P* value
ER				<0.001
Positive	122 (45.69%)	75 (51.02%)	47 (39.17%)	
Negative	112 (41.95%)	66 (44.90%)	46 (38.33%)	
Unknown	33 (12.36%)	6 (4.08%)	27 (22.50%)	
PR				0.109
Positive	66 (24.72%)	42 (28.57%)	24 (20.00%)	
Negative	149 (55.81%)	82 (55.78%)	67 (55.83%)	
Unknown	52 (19.48%)	23 (15.65%)	29 (24.17%)	
HER2				0.035
Negative	141 (52.81%)	73 (49.66%)	68 (56.67%)	
Positive	69 (25.84%)	47 (31.97%)	22 (18.33%)	
Unknown	57 (21.35%)	27 (18.37%)	30 (25.00%)	
Grade				<0.001
I	14 (5.24%)	10 (6.80%)	4 (3.33%)	
II	48 (17.98%)	33 (22.45%)	15 (12.50%)	
III	139 (52.06%)	99 (67.35%)	40 (33.33%)	
Unknown	66 (24.72%)	5 (3.40%)	61 (50.83%)	
Tumor Size				<0.001
Tx	73 (27.34%)	11 (7.48%)	62 (51.67%)	
T1	91 (34.08%)	57 (38.78%)	34 (28.33%)	
T2	70 (26.22%)	55 (37.41%)	15 (12.50%)	
T3	33 (12.36%)	24 (16.33%)	9 (7.50%)	
Lymph node				<0.001
0	84 (31.46%)	59 (40.14%)	25 (20.83%)	
1-3	44 (16.48%)	39 (26.53%)	5 (4.17%)	
4-9	24 (8.99%)	20 (13.61%)	4 (3.33%)	
≥10	13 (4.87%)	11 (7.48%)	2 (1.67%)	
Unknown	102 (38.20%)	18 (12.24%)	84 (70.00%)	
Molecular Subtype*				0.146
Luminal A	78 (29.21%)	41 (27.89%)	37 (30.83%)	
Luminal HER2	32 (11.99%)	23 (15.65%)	9 (7.50%)	
HER2+	32 (11.99%)	21 (14.29%)	11 (9.17%)	
Triple-negative/basal-like	61 (22.85%)	30 (20.41%)	31 (25.83%)	
Unclassified	64 (23.97%)	32 (21.77%)	32 (26.67%)	
CCN1 score				<0.001
0	38 (14.23%)	26 (17.69%)	12 (10.00%)	
1+	59 (22.10%)	49 (33.33%)	10 (8.33%)	
2+	45 (16.85%)	27 (18.37%)	18 (15.00%)	
3+	125 (46.82%)	45 (30.61%)	80 (66.67%)	
CCN1 score				<0.001
Negative (0, 1+, 2+)	142 (53.18%)	102 (69.39%)	40 (33.33%)	
Positive (3+)	125 (46.82%)	45 (30.61%)	80 (66.67%)	

*The immunohistochemical definition of intrinsic molecular subtypes was as follows: luminal A (ER and/or PR positive, HER2-negative), luminal HER2 (ER and/or PR positive, HER2-positive), HER2-overexpression (ER and PR negative, HER2-positive), triple-negative/basal-like (ER, PR, and HER2 negatives).

expression by immunohistochemistry in a BC patient cohort using TMAs of matched pairs of primary tumors (*N*=147) and recurrent/metastatic relapses (*N*=120) (**Table 1**). The intensity

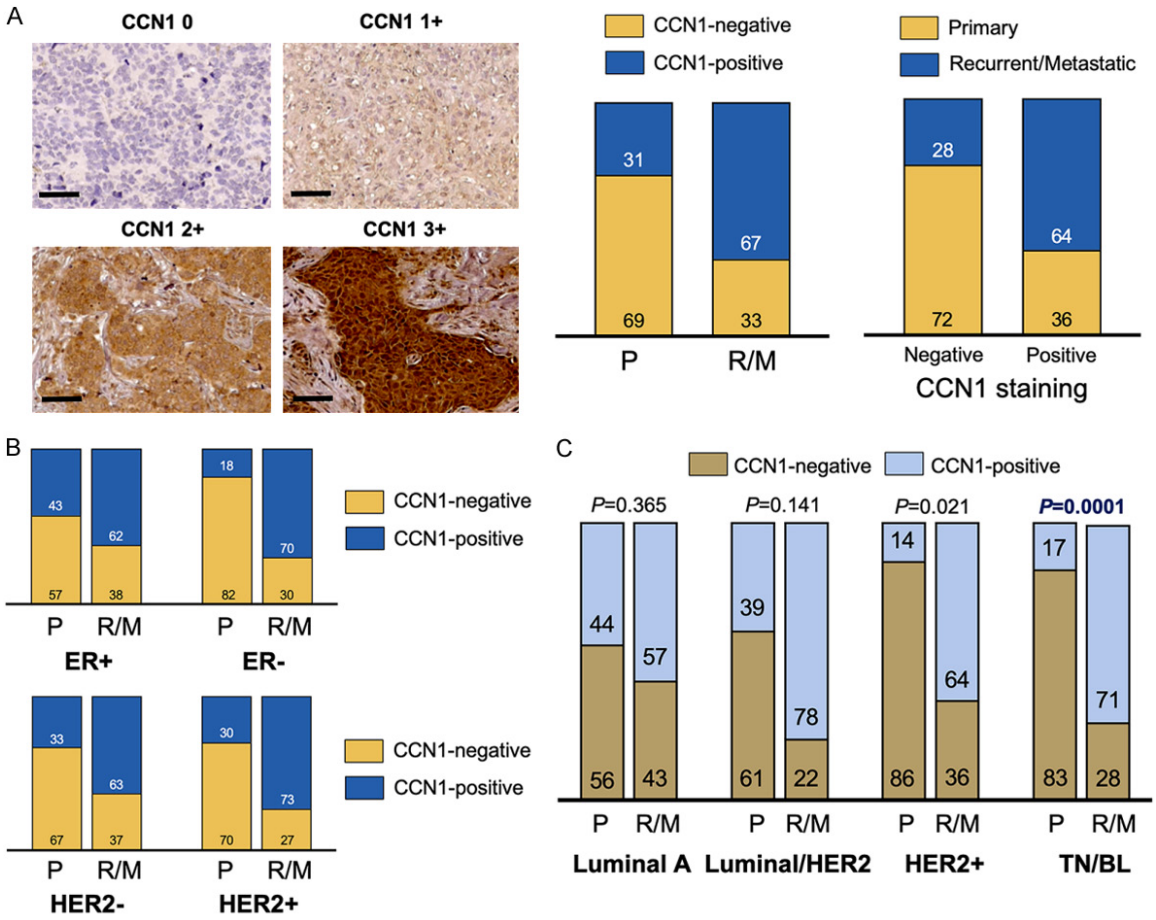

Figure 1. CCN1/CYR61 expression in breast cancer tissues. A. Left. Representative immunohistochemical staining of CCN1/CYR61 protein in breast cancer tissue microarrays. Magnification ×20, scale bar: 50 μm. Right. Stacked bar plots show the percentages of CCN1 staining intensities for the different cohorts of primary (P) and recurrent/metastatic (R/M) tissues. B. Distribution of CCN1 expression status (%) in primary and recurrent/metastatic tissues immunohistochemically-categorized as ER-positive/ER-negative (*top*) and HER2-negative/HER2-positive (*bottom*). C. Distribution of CCN1 expression status (%) in primary and recurrent/metastatic tissues immunohistochemically-categorized as luminal A (ER and/or PR positive, HER2-negative), luminal HER2 (ER and/or PR positive, HER2-positive), HER2-overexpression (ER and PR negative, HER2-positive), triple-negative/basal-like (ER, PR, and HER2 negatives).

of CCN1 staining was initially scored in the entire series using a scale of 0 (negative), 1+ (weak staining), 2+ (intermediate staining), and 3+ (strong staining) (**Figure 1A**, left panels), **Table 1**). Immunostaining scores were then grouped into two categories: negative (scores 0, 1+, and 2+) and positive (scores 3+). The distribution of CCN1-positive samples was notably different between primary and recurrent/metastatic relapses (**Figure 1A**, right panels). Thus, CCN1-positive cases were noted in a significantly higher percentage of recurrent/metastastic relapses (67%) than in primary tumors (33%). When samples were classified according to CCN1 score, 72% of primary tumors were classified as CCN1-negative whereas 64% of recurrent/metastatic relapses were classified as CCN1-positive. When BC tissues were re-classified based on ER expression, there was no difference in the distribution of CCN1-positive staining between ER-positive primary and ER-positive recurrent/metastastic relapses; however, CCN1-positive staining was notably higher in ER-negative recurrent/metastastic relapses than in ER-negative primary tumors (**Figure 1B**, top panel). When BC tissues were re-classified based solely on HER2 overexpression, no differences were noted in the distribution of CCN1-positive staining between primary and recurrent/metastastic relapses regardless

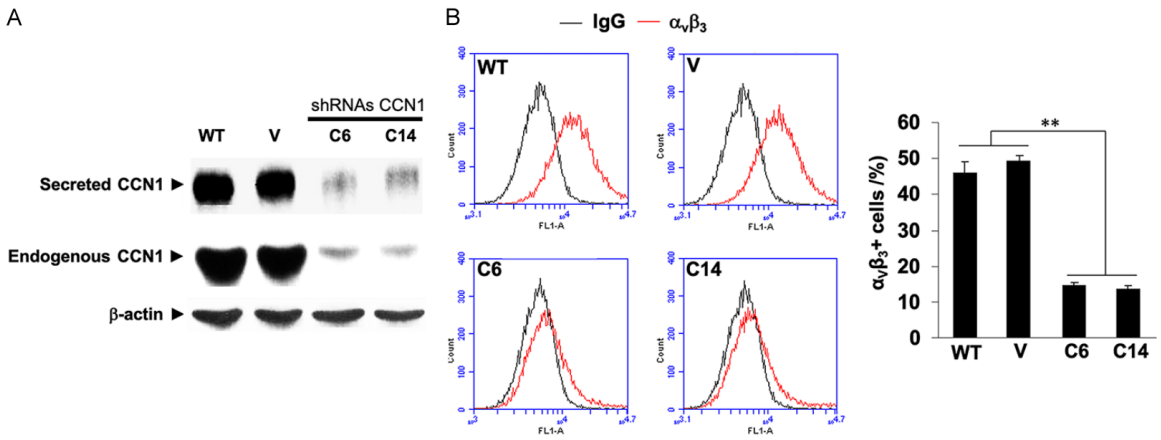

Figure 2. CCN1 depletion suppresses integrin $\alpha_v\beta_3$ overexpression in triple-negative/basal-like BC cells. A. Immunoblotting assessment of secreted and endogenous CCN1 protein in MDA-MB-231 cells transduced with lentiviruses containing an empty vector (V) or a vector containing specific shRNAs against CCN1 (C6 and C14). Blots were re-probed with an antibody for *β*-actin to control for protein loading and transfer. Results are representative of three independent experiments. B. Flow cytometric quantification of $\alpha_v\beta_3$ integrin expression (*top*) and percentage of $\alpha_v\beta_3$-positive cells (*bottom*) in *CCN1*-silenced clones MDA-MB-231 C6 and C14, matched control V, and parental MDA-MB-231 cells. Data presented summarize the mean (*columns*) ± S.D. (*bars*) of three independent experiments (**P<0.005).

of the HER2 expression status (**Figure 1B**, bottom panel). Finally, when BC tissues were reclassified in intrinsic subtypes based on their surrogate immunohistochemical definition (i.e., luminal A, luminal HER2, HER2 overexpression, and triple-negative basal-like), the prevalence of CCN1-positive cases was drastically higher in recurrent tissues (71%) than in primary tumors (17%) from triple-negative/basal-like BC (P= 0.0001; **Figure 1C**).

CCN1 depletion in triple-negative/basal-like BC cells suppresses in vitro cell proliferation and anchorage-independent clonogenic capacity, and inhibits migration

To explore the involvement of CCN1 in eliciting the highly proliferative, clonogenic and invasive phenotype of triple-negative/basal-like BC cells, MDA-MB-231 cells were transduced with a lentiviral vector to stably silence the expression of *CCN1*. Immunoblot analyses confirmed that CCN1 was endogenously overexpressed and secreted with high efficiency in the extracellular milieu of parental MDA-MB-231 cells and empty vector-transduced MDA-MB-231/V cells (**Figure 2A**). By contrast, CCN1 levels were markedly decreased in whole cell lysates and conditioned medium from *CCN1*-silenced MDA-MB-231/C6 and MDA-MB-231/C14 cell clones.

Because the ability of CCN1 to promote cell proliferation and survival in BC cells largely relies on signaling through its receptor integrin $\alpha_v\beta_3$, whose expression is induced by CCN1 itself [23, 27-30], we first evaluated whether depletion of CCN1 changed the expression status of $\alpha_v\beta_3$ in MDA-MB-231 cells. We analyzed cell surface-associated expression of $\alpha_v\beta_3$ by flow cytometry using the anti-$\alpha_v\beta_3$ monoclonal antibody LM609. We observed that $\alpha_v\beta_3$ levels were significantly lower in *CCN1*-silenced C6 and C14 clones than in CCN1-ovexpressing parental and MDA-MB-231/V cells (**Figure 2B**). Anchorage-dependent cell growth was measured using an automated cell counter after 2 and 4 days. Results showed that proliferation was significantly lower in *CCN1*-silenced C6 and C14 clones than in *CCN1*-expressing parental and MDA-MB-231/V cells (**Figure 3A**).

The aggressiveness of cancer cells is closed linked with the acquisition of anchorage-independent growth *in vitro*. In this context, colony formation in soft-agar is the gold-standard assay to measure both anchorage-independent proliferation and cell survival colonization as surrogates of the metastatic capacity of cancer cells [31, 32]. Plated CCN1-expressing MDA-MB-231 and MDA-MB-231/V cells formed an extremely high number (~1,000) of colonies in soft-agar (**Figure 3B**). CCN1 knockdown profoundly reduced the clonogenic capacity of the MDA-MB-231 clonal derivatives C6 and C14, which were virtually unable to grow and survive

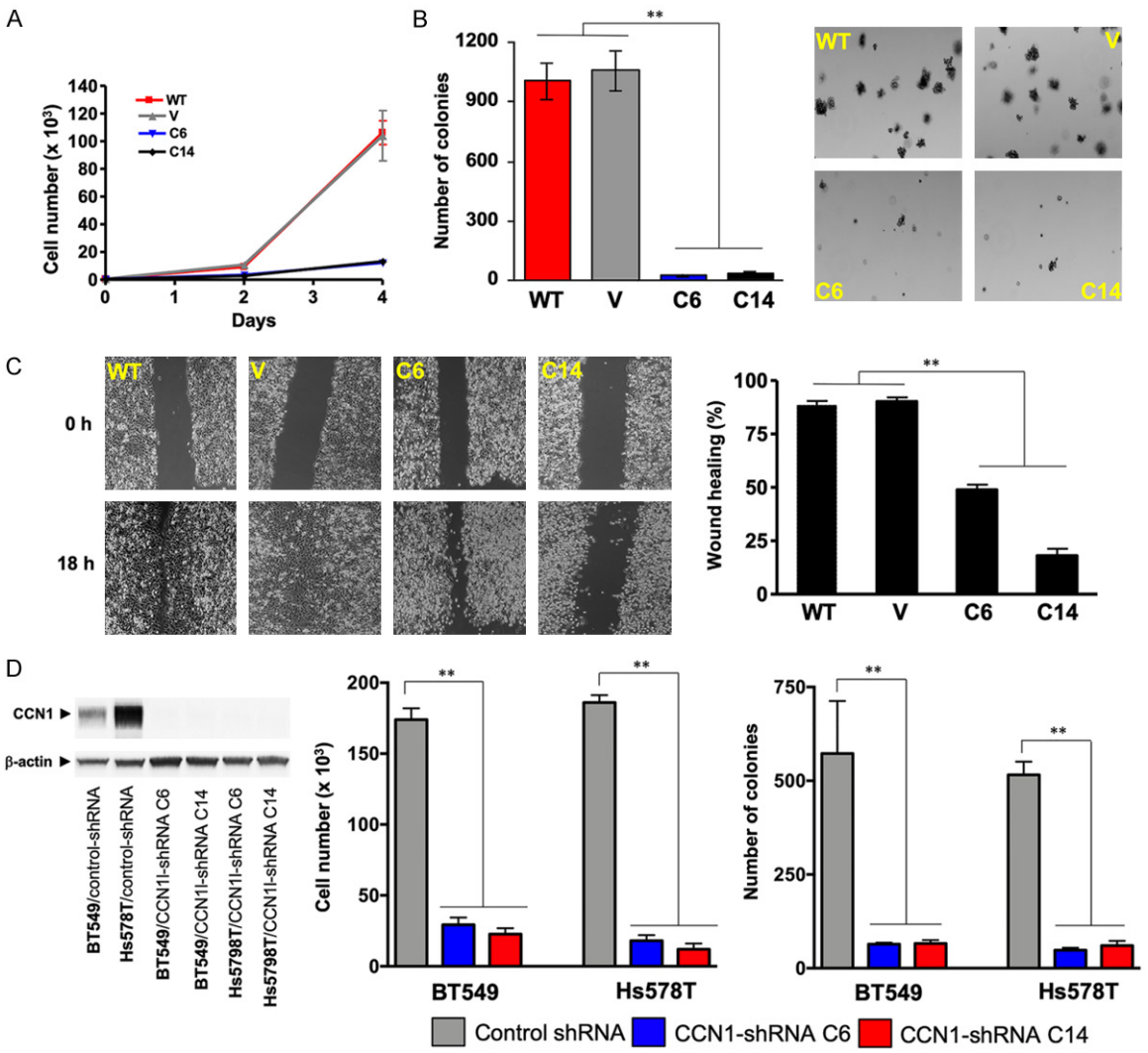

Figure 3. CCN1 depletion suppresses cell proliferation, anchorage-independent cell growth and migration in triple-negative/basal-like BC cells. A. Parental, V, C6, and C14 MDA-MB-231 cells were plated in 24-well plates at 10,000 cells/well and cultured in complete medium. Data presented summarize the mean ± S.D. (*bars*) number of cells $\times 10^4$/well from three independent experiments performed in duplicate and obtained after 0, 3, and 4 days. B. Parental, V, C6, and C14 MDA-MB-231 cells were seeded in soft-agar and the number of colonies (>50 μm) was assessed after 9 days. Data presented summarize the mean (*columns*) ± S.D. (*bars*) of three independent experiments in triplicate (**P<0.005). Representative microphotographs for each cell line are shown on the right. C. Wound healing assays in parental, V, C6, and C14 MDA-MB-231 cells. Confluent cultures were scratched and the closure of the scratch was imaged after 18 h. Quantification (%) of wound closure for each cell line represents the mean (*columns*) ± S.D. (*bars*) of three independent experiments (**P<0.005). D. Left. Immunoblotting assessment of endogenous CCN1 protein in BT-549 and Hs578T cells transduced with lentiviruses containing an empty vector (control shRNA) or a vector containing specific shRNAs against CCN1 (C6 and C14). Blots were re-probed with an antibody for *β*-actin to control for protein loading and transfer. Results are representative of three independent experiments. Right. Cells were plated in 24-well plates at 10,000 cells/well and cultured in complete medium or seeded in soft-agar. Data presented summarize the mean ± S.D. (*bars*) number of cells $\times 10^4$/well from three independent experiments performed in duplicate and obtained after 4 days of anchorage-dependent cell growth or the mean ± S.D. (*bars*) number of colonies (>50 μm) assessed after 9 days of anchorage-independent cell growth.

in an anchorage-independent manner (**Figure 3B**).

Because CCN1 can stimulate metastasis-promoting processes such as $\alpha_v\beta_3$-mediated cell migration, we evaluated whether *CCN1* depletion impacted on the migratory capacity of MDA-MB-231 cells. Confluent monolayers of parental, MDA-MB-231/V, C6, and C14 cells on tissue culture dishes were wounded, and the

relative wound closure area (expressed as the % of the initial scratch) was determined after 18 h. We observed that parental and MDA-MB-231/V cells rapidly closed the wound (>85%) by 18 h, whereas wound closure by C6 (and particularly) C14 cells was very poor (<20%) (**Figure 3C**).

To confirm that the above-mentioned findings were not restricted to a specific triple-negative/basal-like BC cell line (MDA-MB-231), we monitored anchorage-dependent and -independent cell growth in two additional CCN1-overexpressing triple-negative/basal-like BC cell lines (BT-549 and Hs578T) lentivirally transduced to stably silence *CCN1*. CCN1 silencing caused a drastic loss of proliferative capacity and largely suppressed colony formation in soft-agar in highly-aggressive BT-549 and Hs578T triple-negative/basal-like BC cells (**Figure 3D**).

CCN1 depletion inhibits triple-negative/basal-like BC tumor growth in athymic nude mice

To characterize the impact of CCN1 depletion on tumor formation in a biologically relevant microenvironment, we injected parental MDA-MB-231 cells and *CCN1*-silenced clones orthotopically into the mammary fat pads of immunocompromised mice [33, 34]. Mice were monitored weekly for development of primary xenograft tumors during 34 days (**Figure 4A**, top). Injection of parental cells led to the rapid growth of primary mammary fat pad tumors, particularly after day 20 post-injection, generating tumor volumes of approximately 800 mm^3 in a few weeks. Whereas the growth rate of MDA-MB-231/V tumors was indistinguishable from that of MDA-MB-231 parental tumors, tumor progression differed significantly upon injection of *CCN1*-silenced C6 and C14 cells (**Figure 4A**, bottom). The daily growth rate of the C6 and C14 tumors was very poor, and by day 34 the mean tumor volume (200 mm^3) was 25% of that seen in MDA-MB-231 and MDA-MB-231/V groups.

CCN1 depletion enhances E-cadherin expression and reduces microvessel density in triple-negative/basal-like BC xenografts

We finally explored whether correction of CCN1 signaling sufficed to reverse the phenotype of triple-negative/basal-like MDA-MB-231 BC cells. Because disruption of tumor cell adhesion is known to promote angiogenic switches in a variety of human carcinomas including BC [35, 36], we evaluated how CCN1 depletion impacted the expression of epithelial/luminal markers (E-cadherin), microvessel density, and angiogenic factor (VEGF) secretion. Immunohistochemistry of tumor sections from xenografts revealed that E-cadherin, which was completely absent in sections from MDA-MB-231/V cells, was "re-expressed" in those obtained from C6 and C14 primary xenografts (**Figure 4B**). We stained tumor sections with an anti-CD31 (platelet/endothelial cell adhesion molecule; PECAM-1) antibody to report microvessel density (MVD), finding that the mean MVD in MDA-MB-231/V tumor areas was 13 vessels, which was significantly higher than in *CCN1*-silenced tumor sections: 7 and 5 for C6 and C14 tumor areas, respectively (**Figure 4C**). Consistent with this finding, the basal levels of the VEGF secretory isoform, $VEGF_{165}$ from the *CCN1*-silenced C6 and C14 cells (2.9±0.5 and 3.9±0.5 pg VEGF/μg protein, respectively) were significantly lower than those from MDA-MB-231/V cells (7.5±0.49 pg VEGF/μg protein) (**Figure 4C**).

Discussion

Our present findings demonstrate that diminishing CCN1/CYR61 expression suffices to "reverse" the malignant traits that are exacerbated in basal-like/triple-negative breast cancer namely proliferation, migration, clonogenic capacity, tumorigenicity, and angiogenesis. The uncovered driver function of CNN1 in triple-negative/basal-like BC might represent a potential therapeutic opportunity to clinically manage these tumors that, owing to the absence of targeted therapies such as endocrine and anti-HER2 therapy, is limited to chemotherapy after recurrence [1-3].

Clinical analyses of the relationship between CCN1 expression and tumor stage, recurrence, metastasis, and overall survival strongly suggest a BC-promoting role for CCN1 [14-18, 22-26]; however, the relationship between CCN1 levels in the primary lesions of BC and recurrences was unknown. Here, we examined whether CCN1 might be differentially expressed in clinical specimens from primary and recurrence groups of patients with BC. A dramatic increase of the highest CCN1 expression score was only found in recurrent *versus* primary

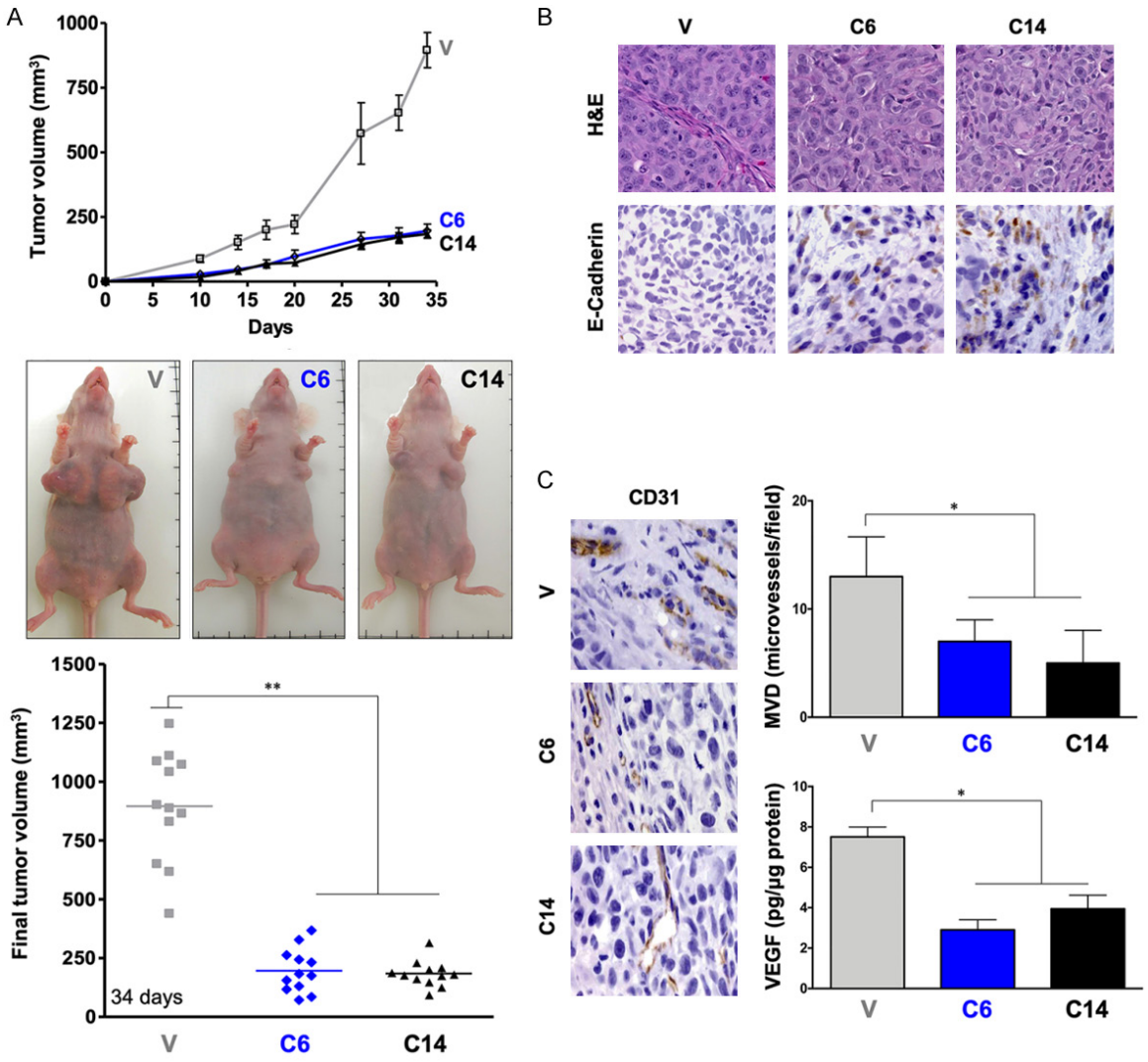

Figure 4. CCN1 depletion reduces tumorigenicity and down-modulates the "angiogenic switch" of triple-negative/basal-like BC in vivo. A. Top. Growth of V, C6, and C14 orthotopic breast tumors in athymic nude mice. Bottom. Representative images of the growth of V, C6, and C14 cells injected in the mammary fat pads of mice are shown. Mean tumor volumes (mm^3) on day 34 of V, C6, and C14 tumors (n=12 mice/experimental group) (**P<0.005). B. Representative hematoxylin and eosin (H&E) stain and immunohistochemical staining for E-cadherin in V, C6, and C14 tumors. C. Representative immunohistochemical CD31 staining (left) and comparison of semi-quantitative assessment of microvascular density (MVD) as numbers of CD31+ vessels/field between V, C6, and C14 tumor groups (*right*) (*P<0.05). The level of $VEGF_{165}$ in the supernatant of V, C6, and C14 cell lines was determined by ELISA, normalized to the amount of protein in the cell extracts, and compared with VEGF secretion in V cells (*P<0.05).

TNBC tumors, and not when recurrent and primary tissues from ER+ and HER2+ tumors were compared. These clinical findings appear to suggest that CCN1 expression plays a role as a molecular regulator of recurrence in TNBC.

Using a combination of *in vitro* and *in vivo* studies, we explored how CCN1 might facilitate the pathogenicity of basal-like/TNBC. In breast epithelial cells, CCN1 can activate the expression of its cognate $\alpha_v\beta_3$ integrin receptor to generate a so-called CCN1-$\alpha_v\beta_3$ autocrine loop [27]. This signaling loop can promote cell proliferation, direct cell migration, enhance cell survival, and boost secretion of VEGF [19, 37, 38]. Our current findings expand this notion by demonstrating that silencing of *CCN1* in archetypal triple-negative/basal-like BC cells suffices to fully interrupt the CCN1/$\alpha_v\beta_3$ feedback loop *in vitro* and *in vivo*. CCN1 depletion leads to the suppression of $\alpha_v\beta_3$ overexpression, thereby generating a dominant negative phenotype capable

of impairing the bioactivity of other growth factors that participate in the high proliferative and migratory capacity of triple-negative/basal-like BC cells. The ability of CCN1 to activate MAPK signaling downstream of $\alpha_v\beta_3$ is likely to be involved in the anti-proliferative and anti-migratory effects of CCN1 silencing in triple-negative/basal-like BC cells [27, 39, 40]. CCN1 depletion also completely blocks the ability of triple-negative/basal-like BC cells to proliferate and form colonies in semi-solid agarose gel. In this setting, *CCN1*-silenced triple-negative/basal-like BC cells fail to propagate in the absence of adherence to the ECM and likely undergo anoikis, a form of apoptosis induced by loss of cell anchorage [41-43]. CCN1, coupled to constitutive activation of $\alpha_v\beta_3$ [44, 45], likely functions as a key protector from anoikis in triple-negative/basal-like BC cells, suggesting that CCN1-dependent cell survival under non-adhesive conditions may facilitate not only primary tumor growth but also tumor cell extravasation and metastatic outgrowth [18]. Our data identify CCN1 as a potential therapeutic target for the management of the key phenotypic traits of triple-negative/basal-like BC cells namely invasiveness, therapeutic resistance, and metastatic dissemination.

Orthotopic xenografting of tumors into the mouse mammary gland allow for the study of BC in a biologically relevant microenvironment and for exploring novel therapies. We found that the sole depletion of *CCN1* sufficed to dramatically reduce tumor burden in a model of triple-negative/basal-like BC tumorigenesis. Because disruption of tumor cell adhesion (e.g., *via* loss of the luminal epithelial marker E-cadherin) is known to promote progression of angiogenic tumors [35, 36], we explored whether CCN1 depletion might reverse the phenotype of triple-negative/basal-like BC *in vivo*. CCN1 silencing partially restored intra-tumoral E-cadherin expression and reversed tumor-associated angiogenesis, as measured by CD31 expression on endothelial cells and VEGF secretion in cancer cells. This is the first report showing that CCN1 depletion reinstates the expression of E-cadherin in E-cadherin-deficient MDA-MB-231 cells, which might promote the transition of triple-negative/basal-like BC cells to a more sessile, less aggressive phenotype *in vivo*. While further studies are needed to investigate the controlling mechanisms, one could speculate that complex epigenetic modifications might underlie CCN1-driven regulation of $\alpha_v\beta_3$ and/or E-cadherin expression in triple-negative/basal-like BC cells [46, 47].

The molecular complexity of triple-negative/basal-like BC poses major challenges for the implementation of targeted therapies and chemotherapy remains the standard therapeutic approach for triple-negative/basal-like BC at all stages. We provide new evidence that CNN1/CYR61-targeted strategies, including the use of potent and selective inhibitors of the integrin $\alpha_v\beta_3$ [48], might be novel therapeutic approaches capable of suppressing the biological aggressiveness of triple-negative/basal-like BC.

Acknowledgements

The authors would like to thank Kenneth McCreath for detailed editing of this manuscript. This work was supported by the NIH National Cancer Institute Grants R01 CA11-8975 and R01 CA116623 (to Ruth Lupu) and by the U.S. Department of Defense (DOD)-Breakthrough 3 Grants BC151072 and BC15-1072P1 (to Ruth Lupu). Work in the Menendez laboratory is supported by the Spanish Ministry of Science and Innovation (Grants SAF2016-80639-P and PID2019-10455GB-I00, Plan Nacional de I+D+I, founded by the European Regional Development Fund, Spain) and by an unrestricted research grant from the Fundació Oncolliga Girona (Lliga catalana d'ajuda al malalt de càncer, Girona). Elisabet Cuyàs holds a research contract "Miguel Servet" (CP20/00003) from the Instituto de Salud Carlos III, Spanish Ministry of Science and Innovation (Spain).

Disclosure of conflict of interest

None.

Address correspondence to: Dr. Ruth Lupu, Mayo Clinic, Department of Experimental Pathology, 200 First Street SW, Rochester, MN 55905, USA. Tel: +1-507-773-0472; Fax: +1-507-284-1678; E-mail: lupu.ruth@mayo.edu; Dr. Javier A Menendez, Catalan Institute of Oncology-Girona Biomedical Research Institute, C/ Dr. Castany s/n, Edifici M2 Parc Hospitalari Martí i Julià, 17190 Salt, Girona, Spain. Tel: +34-872-987-086 Ext. 50; E-mail: jmenendez@idibgi.org

References

[1] Carey L, Winer E, Viale G, Cameron D and Gianni L. Triple-negative breast cancer: disease entity or title of convenience? Nat Rev Clin Oncol 2010; 7: 683-692.

[2] Metzger-Filho O, Tutt A, de Azambuja E, Saini KS, Viale G, Loi S, Bradbury I, Bliss JM, Azim HA Jr, Ellis P, Di Leo A, Baselga J, Sotiriou C and Piccart-Gebhart M. Dissecting the heterogeneity of triple-negative breast cancer. J Clin Oncol 2012; 30: 1879-1887.

[3] Lehmann BD, Pietenpol JA and Tan AR. Triple-negative breast cancer: molecular subtypes and new targets for therapy. Am Soc Clin Oncol Educ Book 2015; e31-39.

[4] Bianchini G, Balko JM, Mayer IA, Sanders ME and Gianni L. Triple-negative breast cancer: challenges and opportunities of a heterogenous disease. Nat Rev Clin Oncol 2016; 13: 674-690.

[5] Pareja F, Geyer FC, Marchiò C, Burke KA, Weigelt B and Reis-Filho JS. Triple-negative breast cancer: the importance of molecular and histologic subtyping, and recognition of low-grade variants. NPJ Breast Cancer 2016; 2: 16036.

[6] Engebraaten O, Vollan HKM and Børresen-Dale AL. Triple-negative breast cancer and the need for new therapeutic targets. Am J Pathol 2013; 183: 1064-1074.

[7] Shi Y, Jin J, Ji W and Guan X. Therapeutic landscape in mutational triple negative breast cancer. Mol Cancer 2018; 17: 99.

[8] Lee A and Djamgoz MBA. Triple negative breast cancer: emerging therapeutic modalities and novel combination therapies. Cancer Treat Rev 2018; 62: 110-122.

[9] Marra A, Viale G and Curigliano G. Recent advances in triple negative breast cancer: the immunotherapy era. BMC Med 2019; 17: 90.

[10] Perbal B. CCN proteins: multifunctional signalling regulators. Lancet 2004; 363: 62-64.

[11] Bleau AM, Planque N and Perbal B. CCN proteins and cancer: two to tango. Front Biosci 2005; 10: 998-1009.

[12] Holbourn KP, Acharya KR and Perbal B. The CCN family of proteins: structure-function relationships. Trends Biochem Sci 2008; 33: 461-473.

[13] Perbal B. The concept of the CCN protein family revisited: a centralized coordination network. J Cell Commun Signal 2018; 12: 3-12.

[14] Tsai MS, Hornby AE, Lakins J and Lupu R. Expression and function of CYR61, an angiogenic factor, in breast cancer cell lines and tumor biopsies. Cancer Res 2000; 60: 5603-5607.

[15] Espinoza I, Liu H, Busby R and Lupu R. CCN1, a candidate target for zoledronic acid treatment in breast cancer. Mol Cancer Ther 2011; 10: 732-741.

[16] Huber MC, Falkenberg N, Hauck SM, Priller M, Braselmann H, Feuchtinger A, Walch A, Schmitt M and Aubele M. Cyr61 and YB-1 are novel interacting partners of uPAR and elevate the malignancy of triple-negative breast cancer. Oncotarget 2016; 7: 44062-44075.

[17] Sánchez-Bailón MP, Calcabrini A, Mayoral-Varo V, Molinari A, Wagner KU, Losada JP, Ciordia S, Albar JP and Martín-Pérez J. Cyr61 as mediator of Src signaling in triple negative breast cancer cells. Oncotarget 2015, 6: 13520-13538.

[18] Huang YT, Lan Q, Lorusso G, Duffey N and Rüegg C. The matricellular protein CYR61 promotes breast cancer lung metastasis by facilitating tumor cell extravasation and suppressing anoikis. Oncotarget 2017; 8: 9200-9215.

[19] Lau LF. CCN1/CYR61: the very model of a modern matricellular protein. Cell Mol Life Sci 2011; 68: 3149-3163.

[20] Kim KH, Won JH, Cheng N and Lau LF. The matricellular protein CCN1 in tissue injury repair. J Cell Commun Signal 2018; 12: 273-279.

[21] Tsai MS, Bogart DF, Li P, Mehmi I and Lupu R. Expression and regulation of Cyr61 in human breast cancer cell lines. Oncogene 2002; 21: 964-973.

[22] Tsai MS, Bogart DF, Castañeda JM, Li P and Lupu R. Cyr61 promotes breast tumorigenesis and cancer progression. Oncogene 2002; 21: 8178-8185.

[23] Menéndez JA, Mehmi I, Griggs DW and Lupu R. The angiogenic factor CYR61 in breast cancer: molecular pathology and therapeutic perspectives. Endocr Relat Cancer 2003; 10: 141-152.

[24] Xie D, Miller CW, O'Kelly J, Nakachi K, Sakashita A, Said JW, Gornbein J and Koeffler HP. Breast cancer. Cyr61 is overexpressed, estrogen-inducible, and associated with more advanced disease. J Biol Chem 2001; 276: 14187-14194.

[25] Mayer S, Erbes T, Timme-Bronsert S, Jaeger M, Rücker G, Kuf F, Stickeler E, Gitsch G and Hirschfeld M. Clinical relevance of Cyr61 expression in patients with hormone-dependent breast cancer. Oncol Lett 2017; 14: 2334-2340.

[26] Jia X, Liu G, Cheng J, Shen Z, Shao Z. CYR61 confers the sensitivity to aromatase inhibitor Letrozole in ER positive breast carcinoma. Curr Cancer Drug Targets 2017; 17: 191-197.

[27] Menendez JA, Vellon L, Mehmi I, Teng PK, Griggs DW and Lupu R. A novel CYR61-triggered 'CYR61-alphavbeta3 integrin loop' regulates breast cancer cell survival and chemosensitivity through activation of ERK1/ERK2 MAPK signaling pathway. Oncogene 2005; 24: 761-779.

[28] Babic AM, Kireeva ML, Kolesnikova TV and Lau LF. CYR61, a product of a growth factor-inducible immediate early gene, promotes angiogenesis and tumor growth. Proc Natl Acad Sci U S A 1998; 95: 6355-6360.
[29] Lau LF and Lam SC. The CCN family of angiogenic regulators: the integrin connection. Exp Cell Res 1999; 248: 44-57.
[30] Lau LF. Cell surface receptors for CCN proteins. J Cell Commun Signal 2016; 10: 121-127.
[31] Pampaloni F, Reynaud EG and Stelzer EH. The third dimension bridges the gap between cell culture and live tissue. Nat Rev Mol Cell Biol 2007; 8: 839-845.
[32] Borowicz S, Van Scoyk M, Avasarala S, Karuppusamy Rathinam MK, Tauler J, Bikkavilli RK and Winn RA. The soft agar colony formation assay. J Vis Exp 2014; 92: e51998.
[33] Iorns E, Drews-Elger K, Ward TM, Dean S, Clarke J, Berry D, El Ashry D and Lippman M. A new mouse model for the study of human breast cancer metastasis. PLoS One 2012; 7: e47995.
[34] Zhang GL, Zhang Y, Cao KX and Wang XM. Orthotopic injection of breast cancer cells into the mice mammary fat pad. J Vis Exp 2019.
[35] Derksen PW, Liu X, Saridin F, van der Gulden H, Zevenhoven J, Evers B, van Beijnum JR, Griffioen AW, Vink J, Krimpenfort P, Peterse JL, Cardiff RD, Berns A and Jonkers J. Somatic inactivation of E-cadherin and p53 in mice leads to metastatic lobular mammary carcinoma through induction of anoikis resistance and angiogenesis. Cancer Cell 2006; 10: 437-449.
[36] Ceteci F, Ceteci S, Karreman C, Kramer BW, Asan E, Götz R and Rapp UR. Disruption of tumor cell adhesion promotes angiogenic switch and progression to micrometastasis in RAF-driven murine lung cancer. Cancer Cell 2007; 12: 145-159.
[37] Espinoza I, Menendez JA, Kvp CM and Lupu R. CCN1 promotes vascular endothelial growth factor secretion through alphavbeta 3 integrin receptors in breast cancer. J Cell Commun Signal 2014; 8: 23-27.
[38] Menendez JA, Vellon L, Espinoza I and Lupu R. The metastasis inducer CCN1 (CYR61) activates the fatty acid synthase (FASN)-driven lipogenic phenotype in breast cancer cells. Oncoscience 2016; 3: 242-257.
[39] Vellon L, Menendez JA and Lupu R. A bidirectional "alpha(v)beta(3) integrin-ERK1/ERK2 MAPK" connection regulates the proliferation of breast cancer cells. Mol Carcinog 2006; 45: 795-804.
[40] Vellon L, Menendez JA and Lupu R. AlphaVbeta3 integrin regulates heregulin (HRG)-induced cell proliferation and survival in breast cancer. Oncogene 2005; 24: 3759-3773.
[41] Guadamillas MC, Cerezo A and Del Pozo MA. Overcoming anoikis--pathways to anchorage-independent growth in cancer. J Cell Sci 2011; 124: 3189-3197.
[42] Taddei ML, Giannoni E, Fiaschi T and Chiarugi P. Anoikis: an emerging hallmark in health and diseases. J Pathol 2012; 226: 380-393.
[43] Celià-Terrassa T and Kang Y. Distinctive properties of metastasis-initiating cells. Genes Dev 2016; 30: 892-908.
[44] Dolinschek R, Hingerl J, Benge A, Zafiu C, Schüren E, Ehmoser EK, Lössner D and Reuning U. Constitutive activation of integrin alphavbeta3 contributes to anoikis resistance of ovarian cancer cells. Mol Oncol 2021; 15: 503-522.
[45] Paoli P, Giannoni E and Chiarugi P. Anoikis molecular pathways and its role in cancer progression. Biochim Biophys Acta 2013; 1833: 3481-3498.
[46] Deb M, Sengupta D and Patra SK. Integrin-epigenetics: a system with imperative impact on cancer. Cancer Metastasis Rev 2012; 31: 221-234.
[47] Madrazo E, Conde AC and Redondo-Muñoz J. Inside the cell: integrins as new governors of nuclear alterations? Cancers (Basel) 2017; 9: 82.
[48] Haddad T, Qin R, Lupu R, Satele D, Eadens M, Goetz MP, Erlichman C and Molina J. A phase I study of cilengitide and paclitaxel in patients with advanced solid tumors. Cancer Chemother Pharmacol 2017; 79: 1221-1227.